Chapter 5

Studies on effect of cuo addition on mechanical properties and in vitro cytocompatibility in 1393 bioactive glass scaffold

5.1 INTRODUCTION

Bone diseases like osteoporosis and fluorosis (caused due to fluorine or its compounds) where bone strength significantly decreases and the weak bones lead to fatal injury even after a minor incident is a serious concern in recent times (Aaseth et al., 2012). Due to the high mechanical strengths and nearly bio-inert nature, the metallic implants were used to repair/ replace such diseased/fractured bones is a matter of fact, for decades (Boyan et al., 1996). However, metallic implants often require replacement surgery because they release toxic materials after a certain period due to several electrochemical changes. The corrosion of metals in physiological fluid leading to the formation of micro debris, and therefore, could cause severe damage to the prosthetic region (Puleo and Nanci, 1999, Jacobs et al., 1998, Brown et al., 2015, Merritt and Brown, 1996). Moreover, the risks of metallic-implants failure persist due to the mismatch in thermal expansion coefficient and stiffness with the bone (Doiphode et al., 2011, Woesz, 2008). Furthermore, the shortcomings in polymeric biomaterials (mechanical strengths), *Autografts*, and *Allografts* (aftermath morbidity and pathogenic transfer) limited them from being implant materials (Goldstein et al., 1999, Kneser et al., 2002, Griffith, 2000, Borden et al., 2003, Liu et al., 2013a, Bi et al., 2013). However, the bioactive glasses are most suited in replacement or repairing such defective bones due to their bioactivity and biocompatibility. The term ‘bioactive’ is used to describe the unique ability of these materials to bond with soft and hard bone tissues by

means of series of reactions, which produces a strong, compliant interface between the implant and the host tissues (LL, 1998). Nevertheless, the porous material templates are often considered to be the most basic requirements for formation of new blood vessels, their proliferation, differentiation and tissue ingrowths (Bose et al., 2012). However, the porosity can be produced by several techniques as described elsewhere (Kargozar et al., 2018, Chen et al., 2006, Jones and Hench, 2003, Maquet et al., 2003, Ma and Zhang, 2001, Bi et al., 2013, Gerhardt and Boccaccini, 2010). Herein, the three dimensional (3D) porous 1393 bioactive glass scaffold mimicking spongy bone was prepared by replicating the sacrificial porous PU (polyurethane) template. The 1393 bioactive glass is the modified version of most popular 45S5®. Typically it consists of 53% SiO_2, 20% CaO, 6% Na_2O, 4% P_2O_5, 12% K_2O and 5% MgO (wt%). There are some advantages of 1393 bioglass over 45S5®. 1393 has the facile viscous flow behavior than that of 45S5. Unlike 45S5®, 1393 could not be transformed into polycrystalline form easily, as the latter has fewer crystallization tendency during sintering (Fu et al., 2008, Deliormanlı, 2015). Also 1393 can be pulled easily into particles or short to long range fibers without devitrification and it has better bioactivity than that of 45S5® (Fu et al., 2008, Fu et al., 2007). Inorganic metallic elements or their oxides often use to biomaterials for the betterment of biological responses as well as physicochemical or mechanical behavior (Vyas et al., 2015, Vyas et al., 2016, Ershad et al., 2018). Trace elements like Zn, Sr, K, Li, Fe, Mn, Co, Cu found in bone matrix (higher in trabecular part than cortical part) and collagen play an important role in increasing bone density, enhancing physico-mechanical strength (Takata et al., 2005, Arepalli et al., 2016). The delivery of copper ions from bioactive scaffold materials to stimulate angiogenesis is attracting substantial attention in current years (Giacomelli et al., 2015). Studies have shown the ability of Cu ions to promote in vitro endothelial cells proliferation and to

stimulate VEGF gene expression to promote wound healing (Finney et al., 2009, Gérard et al., 2010, Hu, 1998, Sen et al., 2002, Frangoulis et al., 2007). Previous researches suggest that lack of Cu ions could suppress formation of blood vessels (Raju et al., 1982, Alessandri et al., 1984). Also Cu has found in enhancing osteogenic effects like differentiation of mesenchymal stem cells (MSC) and osteoblastic cells (Wu et al., 2013, Rodriguez et al., 2002). However, there are several researches, where the authors reported copper as a non-cytotoxic up to a certain limit. Yinan Lin et.al claimed that more than 0.8wt% CuO is toxic and detrimental for bone regeneration (Lin et al., 2016), while Hui Wang et.al proclaimed scaffolds doped with 3.0 wt% CuO showed a significantly better bone regeneration and angiogenesis capacity when compared to the undoped glass scaffolds (Wang et al., 2014).

However, in our current investigation, we replicated 3 dimensional porous 1393 glass structure using packaging polyurethane foam. The observed mean apparent porosities of the scaffolds were 45.8-47.3% (Mean ±SD; n=3) measured by Archimedes's principle. We have studied the effects of CuO on mechanical properties and chemical durability after immersion in SBF. Further, we have extensive *in vitro* cell culture studies like cell viability, growth inhibition and apoptosis for better conclusions. The Hemolytic assay was used to check the compatibility of the scaffolds with RBC and WBC.

5.2 MATERIALS AND METHOD

5.2.1 Preparation of Scaffolds

Chemical compositions for preparation of scaffolds are tabulated below (*Table 5.1*). Briefly, the proportionate amount of anhydrous analytical reagent (AR) grade quartz, sodium carbonate, calcium carbonate, potassium carbonate, magnesium oxide, cupric oxide

and ammonium dihydrogen orthophosphate (Assay: 98–99.9%, Loba chemie, Mumbai, India), were weighed and homogenously mixed for at least 30 minutes prior melting.

Table 5.1: Chemical composition of scaffolds (mol%)

Scaffolds	SiO_2	CaO	Na_2O	K_2O	MgO	P_2O_5	CuO
1393	54.65	22	6	7.9	7.7	1.75	0
1393-1Cu	53.65	22	6	7.9	7.7	1.75	1
1393-2Cu	52.65	22	6	7.9	7.7	1.75	2
1393-3Cu	51.65	22	6	7.9	7.7	1.75	3

The weighed batches were melted in an electric furnace at 1330±10 ^{0}C in Platinum crucibles. The glasses after being air quenched at room temperature, were crushed, ground and passed through a 60μm mesh. The powdered samples were then ball milled for additional 12h by alumina balls (Alcoa, USA) as grinding media and ethanol (Merck, Germany) as liquid media to ensure enough fine (<20μm) particles. Then, a slurry was prepared by mixing 40 vol% of the powdered samples to '20 vol% of millipore double distilled water + 40 vol% ethyl alcohol' and 1-2 wt% (of dry weight of powder) PVA (binder cum deflocculant) and kept for stirring.

Polyurethane packaging (PU) foam with 40-45 pores per inch (PPI) were cut into two standard dimensions of 25mm×10mm×10mm and 10mm×10mm×10mm. The PU foams were slurry infiltrated by dipping them into the slurry. Additionally, the porous foams and surfaces were evenly coated with the help of syringe. Slurry infiltrated foams were then allowed to soak for 1h at 80 ^{0}C. Excess slurry was cut out from the surfaces and were dried at 150 ^{0}C for additional 24h. Coated foams were then subjected to a controlled heat tube furnace, maintaining the heating rate 2 ^{0}C/minute up to 300 ^{0}C and 0.5 ^{0}C/minute up to 700

^{0}C. Heating was hold at 300 C for 1h to remove the binder (PVA ~285℃) and 700 ^{0}C for 2h to sinter (densification and strengthen) the scaffolds.

5.2.2 Preparation of SBF

The SBF solution was prepared according to the procedure described by Kokubo et al. (Kokubo and Takadama, 2006). However, the composition and preparation of the SBF was briefly described in the previous chapter (chapter 4). According to Oyane and Takadama the SBF solution is so far the best solution for *in vitro* measurement of apatite-forming ability in implant materials (Oyane et al., 2003, Takadama et al., 2004).

5.2.3 Evaluation of bioactivities after SBF treatment

In vitro bioactivities (formation of HA layered surface) were evaluated using FTIR, SEM and XRD and pH analysis. For each test, separately .25 gm of each sample (powder for XRD, FTIR and pH, scaffolds for SEM) was immersed in 25ml (10mg/ml) of SBF solution and was then kept for soaking in a bacteriological incubator (Ikon, India) at 37±2 ^{0}C for 1,3,5,9 and 15 days to ensure different levels HA formation. After soaking, the powder were filtered, rinsed with Millipore double distilled water and dried in an oven (Ikon, India) at 100 ^{0}C for 2h. The formation of hydroxyapatite (HA) layer on the surface of the samples was determined by the above mentioned techniques.

5.2.3.1 pH behavior

Changes in pH behavior were evaluated after immersing the finely ground scaffolds to SBF (10 mg/ml) as an indication of formation of Hydroxyapatite. pH of the SBF solution was measured using a digital pH meter (Universal Bio microprocessor, India) and the changes are recorded for 1, 3, 5, 9 and 15 days.

5.2.3.2 XRD

To corroborate the formation of crystalline phases (HA and other crystalline phases) after sintering as well as after SBF treatment, the bioactive scaffolds were ground to less than 100 μm and they were subjected to X-ray diffractometer (RIGAKU-Miniflex II diffractometer adopted Cu-K_α radiation (λ = 1.5405 Å) with a tube voltage of 40 kV and current of 35 mA in a 2θ range between 10° and 80° keeping the scanning rate .02°/sec. The International Centre for Diffraction Data (ICDD) cards were used as a tool for identifying the peaks.

5.2.3.3 FTIR

Different functional groups of bioactive glass scaffolds were assessed by subjecting the finely ground powdered samples to a Fourier transform infrared (FTIR) spectrometer (BRUKER Tensor, 27 FTIR, Germany) in the frequency range of 4000–400 cm^{-1}.

5.2.3.4 SEM

Morphological characterization of the scaffolds with respect to surface modifications was performed using scanning electron microscopy (SEM). A set of porous scaffolds were selected and analyzed using a scanning electron microscope (SEM) (Inspect S50, FEI), before and after soaking in SBF for 15 days. Prior analysis, the scaffold surfaces were plasma coated with a very thin gold layer by sputtering (for 40 sec).

5.2.4 Mechanical properties

5.2.4.1 Relative Density and Apparent Porosity and True porosity

The apparent specific gravity or relative density (RD) and the apparent porosity (AP) of the bioactive scaffolds were determined by Archimedes' principle (ASTM C20-00) with water

as buoyant by the following formulas. True specific gravity was also measured using SG bottles (25 ml) in accordance with ASTM D167-12a to determine the true porosity.

$$RD = \frac{w_a}{w_a - w_c}$$

$$\% AP = \frac{w_b - w_a}{w_b - w_c} \times 100$$

$$\% TP = \left\{1 - \frac{RD}{True\ specific\ gravity}\right\} \times 100$$

Where, w_a= dry weight of the sample in air; w_b= soaked (water saturated) weight of the sample in air; and w_c= suspended weight of the sample in water.

5.2.4.2 Compressive and Flexural strength

The compressive and 3 point bend (flexure) tests for the scaffolds were determined using Universal Testing Machine (H10KL, Tinius Olsen, USA). Maintaining the crosshead speed 0.5 mm/min, the as fabricated 1393 scaffolds of dimensions 10×10×10 mm^3 and 25×10×10 mm^3 were brought under a 10 KN load cell to measure the compression and flexural strength respectively. Flexural strength, according to ASTM C1674-11 has been calculated by the equation

$$\sigma = \frac{3Pl}{2bd^2}$$

Where, P = Applied load (N); l = Outer span length of the specimen (mm); b = specimen width (mm); d = thickness of the sample (mm).

5.2.4.3 Modulus of elasticity

Elastic modulus for compression of the 1393 scaffolds has been calculated by the following formula

$$F = \frac{Compressive\ stress}{Strain\ under\ compression} = \frac{\frac{F}{A}}{\frac{\Delta l}{l}} = \frac{Fl}{A\Delta l}$$

Where, F = Applied load (N); A = cross section of specimen (mm^2); l = specimen length (mm); Δl = change in length (mm).

5.2.5 Chemical durability

Chemical durability is the measure of resistance offered by a *glass* towards attack by aqueous solutions and atmospheric agents. Although there is no absolute or explicit *measure of chemical durability*, weight loss techniques had previously been used to measure the durability of a glass (Paul, 1977). From the definition it can be conferred that the lesser the weight loss of the glass sample better is the chemical durability. Weight loss of the scaffolds was calculated by the formula

$$\%\ \text{Weight loss} = \frac{W_i - W_f}{W_i} \times 100$$

Where, W_i = initial weight, W_f = final weight

5.2.6 Physiological and hemolytic evaluation

Cell culture

Human squamous cell SCC-25 from American Type Culture Collection (ATCC), Manassas, USA was maintained in RPMI 1640 (Invitrogen, Carlsbad, CA) supplemented

with 10% fetal bovine serum (Hyclone, Logan, UT), 100 U/ml penicillin and 100 µg/ml streptomycin (Invitrogen, Carlsbad, CA), considered as complete medium.

5.2.6.1 *In vitro* cell viability assay

Colorimetric XTT (sodium 3-[1-(phenylaminocarbonyl)-3,4-tetrazolium]-bis(4-methoxy-6-nitro) benzene sulfonic acid hydrate) assay; (Roche Molecular Biochemicals, India) was used to study the bioactive scaffolds (1393, 1393-1Cu, 1393-2Cu, 1393-3Cu) on viability of the scuamous cell (SCC-25). SCC-25 cells (5×10^3 cells/well) were added in a 96- well plate and exposed to a series of concentrations (5, 10, 20 & 50 mg/ml) of scaffold materials and incubated at 37°C for 48h in a humidified 5% CO_2 atmosphere. Optical Density (OD) at wavelength 450nm was calculated using Synergy HT Multi-Mode Micro plate Reader (BioTek, USA) by the formula.

$$\% \text{ Cell viability} = \frac{\text{Experimental OD}_{450}}{\text{Control OD}_{450}} \times 100$$

Where, OD_{450} is the optical density at wavelength 450nm

5.2.6.2 In-vitro cell proliferation

Growth inhibitory potential of 1393 scaffolds along with their copper containing derivatives was studied against the squamous cell (SCC-25) by MTT assay (Promega, USA) using a tissue culture plate of having 96 wells, each containing 5×10^3 cells. After incubating for 18 hours in a 5% CO_2 atmosphere @37℃, the plates were exposed to the scaffolds materials to check their cell proliferative potential. The percent growth inhibition is calculated by the formula

$$\% \text{ Growth inhibition} = \left[1 - \frac{\text{Experimental } OD_{570}}{\text{Control } OD_{570}}\right] \times 100$$

Where, OD_{570} is the optical density or absorbance at wavelength 570nm

5.2.6.3 Apoptotic assessment

Scaffolds incorporated with varying concentrations of CuO were assessed by apoptotic detection assay; FITC conjugated Annexin V. Apoptotic cells, after 18 hours of incubation were analyzed with stained FITC conjugated Annexin V and propidium iodide (PI) in cold PBS for 20 min. After washing the cells in Annexin buffer, the FITC conjugated Annexin V positive cells were mounted on microscope (using a drop of mounting medium to lessen fluorescence photo bleaching) and measured using fluorescence microscope (Nikon Eclipse 80i, Nikon, Japan).

5.2.6.4 Hemolytic assessment

To test the hemolysis, the blood sample along with the scaffold materials was incubated for 4 hours. Hemolysis assay was prepared in accordance with the standard protocol i.e. an aliquot blood sample was centrifuged at 600×g for 10 min for each assay followed by dilution of 25 µl supernatant aliquot with 225 µl Drabkin's reagent (Sigma) in a 96 well plate and homogenization for 2 minutes under lateral agitation (300 rpm). OD was measured using Synergy HT Multi-Mode Micro plate Reader (BioTek, USA). Hemoglobin was determined by measuring the OD of the blood after a hundred fold dilution in Drabkin's reagent, at a wavelength of 540nm. Saponin (2 mg/ml) and PBS were used as positive and negative control respectively. The percent hemolysis was calculated as

$$\% \text{ Hemolysis} = \frac{\text{OD540}_{\text{sample}} - \text{OD540}_{\text{negetive control}}}{\text{OD540}_{\text{positive control}} - \text{OD540}_{\text{negetive contol}}} \times 100$$

5.2.7 Statistical analysis

Unpaired student's t-test or one way ANOVA followed by Tukey's post hoc test was performed while comparing between two groups. Each experiment was performed in triplicate and the data were presented as mean ± SD (standard deviation). Differences were considered significant for 'p' value less than 0.05 (*) or 0.01(**) and 0.001(***).

5.3 RESULTS

5.3.1 Evaluation of bioactivity

5.3.1.1 pH behavior in SBF

Fig 5.1 shows that the change in pH after soaking the samples in SBF for different time periods. The pH values of the SBF solution were taken at 48h interval for first five days and were found increasing with increase in number of days up to day3. The day3 mean (n=3) pH @ 37℃ were found to be increased to 8.6, 8.7, 8.8 and 8.9 from 7.4 (day0) for the corresponding scaffolds. After that, there was a sharp decrease in pH (after day3) and the decreasing rate was reduced with increasing number of days and almost become constant as it tended to day15 and thereafter (not shown). It was also observed that the increasing CuO percentage in the scaffolds has resulted in increasing the pH.

5.3.1.2 XRD

Fig 5.2(A) & Fig 5.2(B) represents the XRD pattern of 'sintered only' (700℃) and 'soaked in SBF for 5 days' scaffolds, while Fig 5.3(A) to Fig 5.3(D) correspond to 'soaked in SBF'

scaffolds only. Fig 5.2(A) indicates that there was no intense peaks but a bump at 2θ=20-30°. However, intense peaks were observed for the soaked in SBF glass samples. Furthermore, peak intensities were varied over immersion time, as shown in Fig 5.3. Nonetheless, after a continuous increase up to day5, a decrease and the gradual broadening of the intensities were observed. Results also illustrate that the peak intensities appeared almost nil at day15.

5.3.1.3 Surface morphology evaluation

Fig 5.4(A, B) and Fig 5.5 represent the SEM micrographs of pre and post SBF treated (15days @37°C) scaffolds. The results reveal many an information regarding surface morphology for the 'soaked in SBF' scaffolds. However, the morphological analysis confirms the agglomerated HA like clusters distributed through the SBF soaked scaffolds' surfaces.

5.3.1.4 FTIR

FTIR analysis of the SBF treated scaffolds (Fig 5.6) shows the distinctive resonance peaks at different wavenumbers. However, the characteristic resonance peaks were found at 450 cm^{-1}, 566 cm^{-1}, 795 cm^{-1} and 1035 cm^{-1}. Moreover, the results indicate that the resonance peaks at 566 cm^{-1} and 1036 cm^{-1} were exclusively explicit for SBF treated samples and intensified further with the increasing number of days of immersion. There are some mild intense peaks between 1400-1700 cm^{-1} and a broadened band at 2800-3700 cm^{-1} as well.

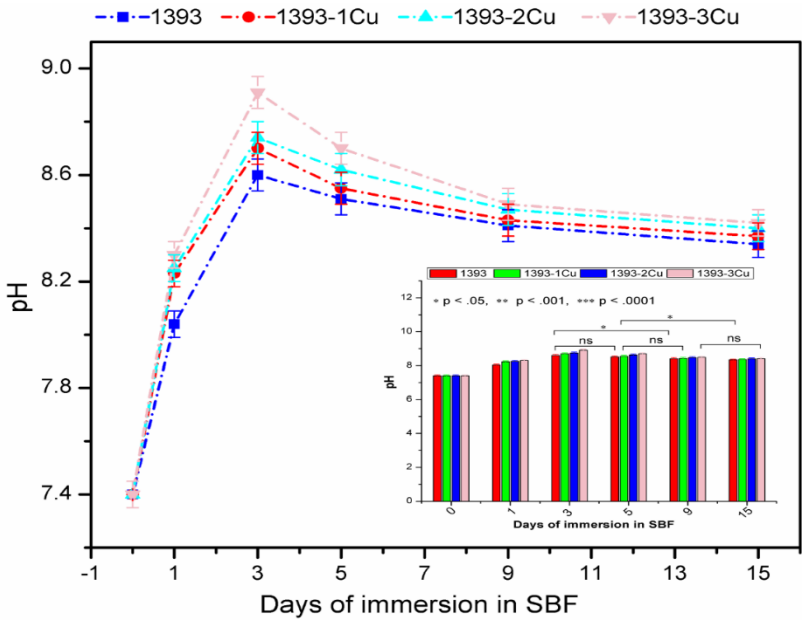

Fig 5.1 pH as a function of materials incubation time. Statistical analysis shows not significant (ns), significant (p<.05) and highly significant (p<.01 and p<.001) difference in pH and weight after Cu addition.

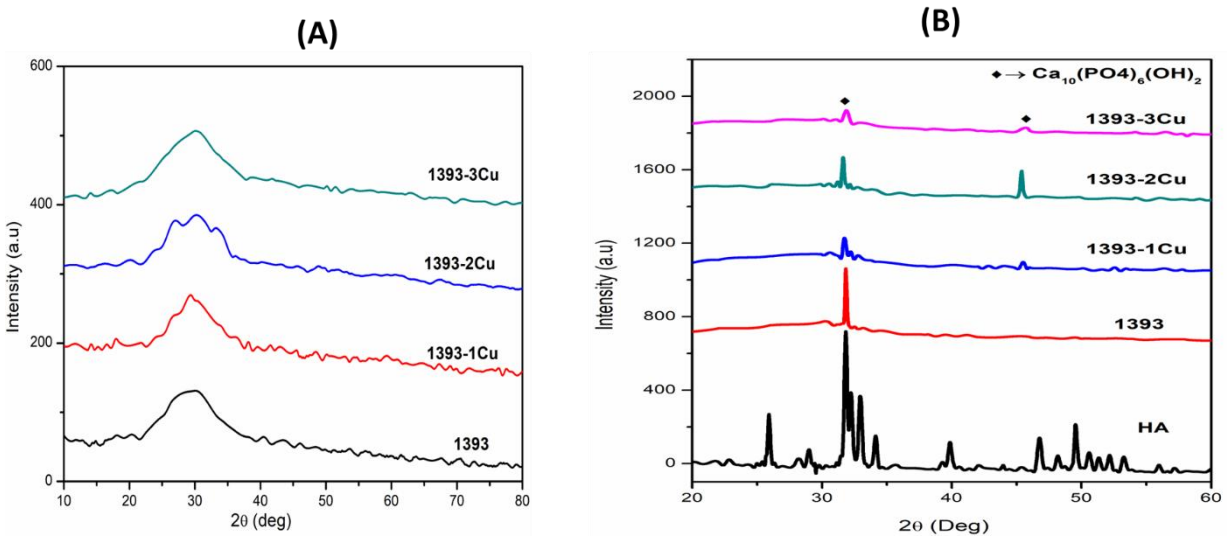

Fig 5.2 X-ray diffraction pattern of 1393 and their Cu derivatives for **(A)** as sintered (700℃) and **(B)** soaked in SBF for 5 days

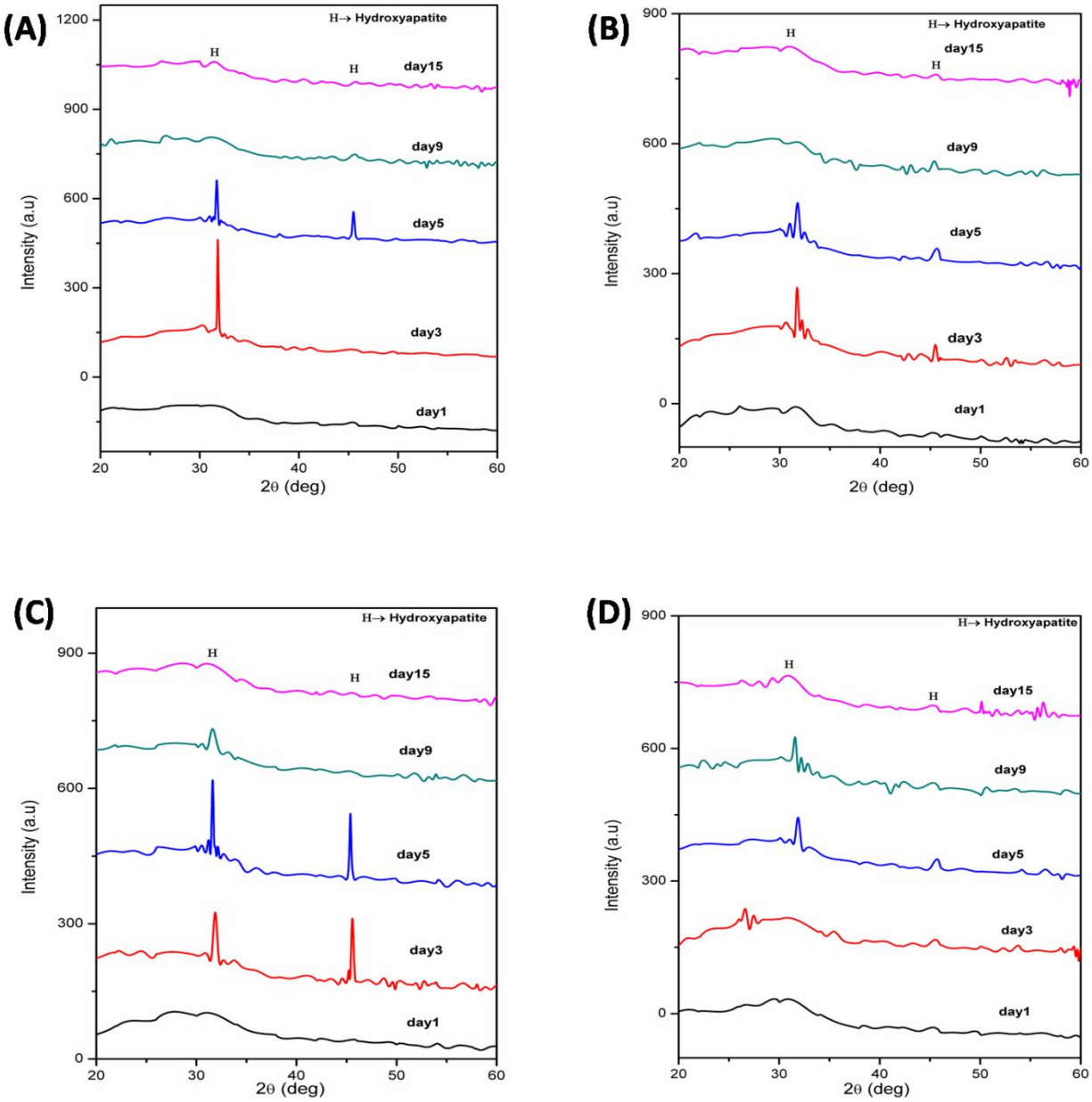

Fig 5.3 X-ray diffraction pattern for **(A)** 1393 **(B)** 1393-1Cu **(C)** 1393-2Cu **(D)** 1393-3Cu of 1393 derived scaffolds

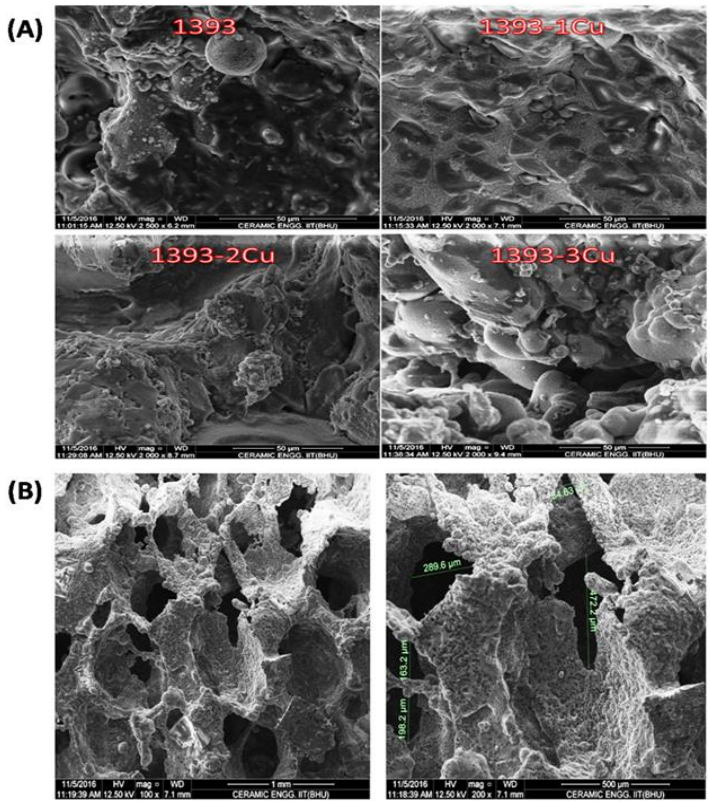

Fig 5.4 SEM micrographs for **(A)** 1393 and their copper derivatives before immersion in SBF and **(B)** Scaffold showing porosity.

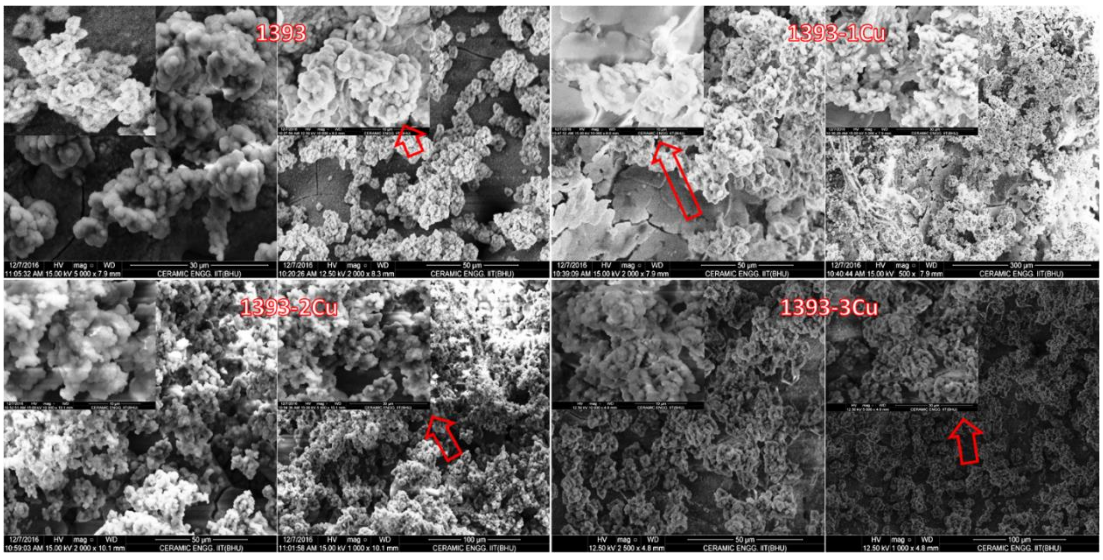

Fig 5.5 SEM micrographs of the 1393 bioactive glass scaffolds after immersion for 15 days in SBF. Different magnification image showing fine cluster of HA crystals

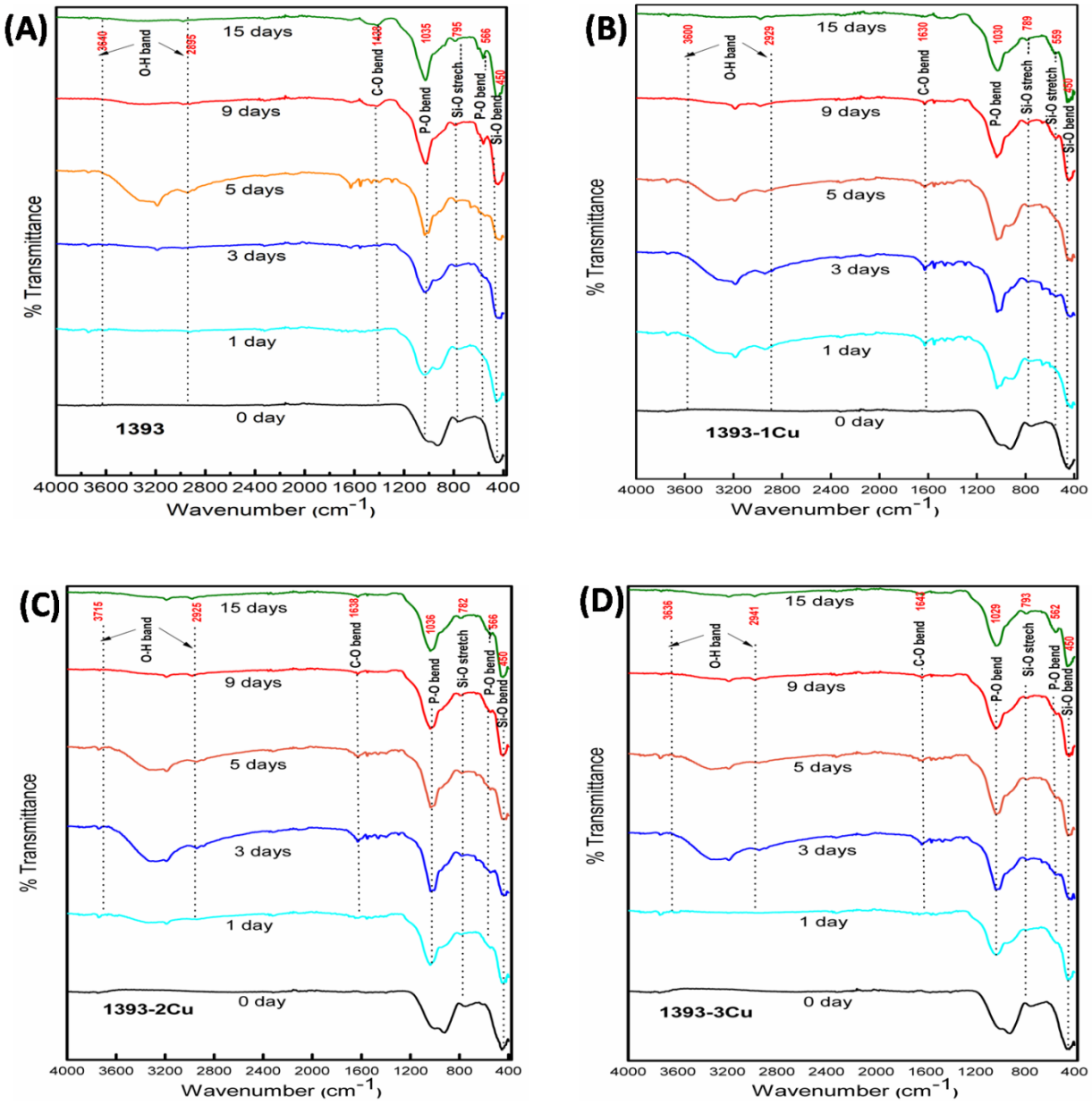

Fig 5.6 FTIR transmittance spectral analysis for **(A)** 1393 **(B)** 1393-1Cu **(C)** 1393-2Cu **(D)** 1393-3Cu of prior (day0) and post (day1 to 15) SBF treated samples

5.3.2 Mechanical behavior

Total or true porosity (TP) along with apparent porosity (AP) and relative density were found in the range of 75-76%, 45-48% and 0.66-0.68 gm/cc respectively. The porosity and

density were calculated for the 'sintered only' porous samples by taking the average of five samples of each kind (mean ± SD) and results were tabulated as 'mean ±SD' (*Table 5.3*)

Table 5.2: Mechanical and physical properties of the 1393 derived scaffolds

Scaffolds	**RD**		**% AP**		**% TP**	
	Mean	SD (±)	Mean	SD (±)	Mean	SD (±)
1393	0.67	0.01	45.8	1.5	75.1	2.4
1393-1Cu	0.66	0.02	45.0	2.0	75.6	2.7
1393-2Cu	0.67	0.04	47.8	1.3	75.4	5.5
1393-3Cu	0.68	0.05	47.3	2.4	75.1	5.1

We have tested 3PT flexure, compression and modulus of elasticity of the corresponding scaffolds and the results were cumulated and reported. The compressive strength found for the 1393 scaffold was 6.9 MPa, while for the CuO substituted scaffolds (1393-1Cu, 1393-2Cu, 1393-3Cu) they were increased to 7.1, 7.3 and 7.6 MPa (Fig 5.7(A)) (taking the mean value of five such samples of each scaffold). The flexural strengths observed for the corresponding scaffolds were 0.5-0.78 MPa (Fig 5.7(A)). Elastic moduli calculated from the compression tests were within 1.34-1.42 GPa (Fig 5.7(B)).

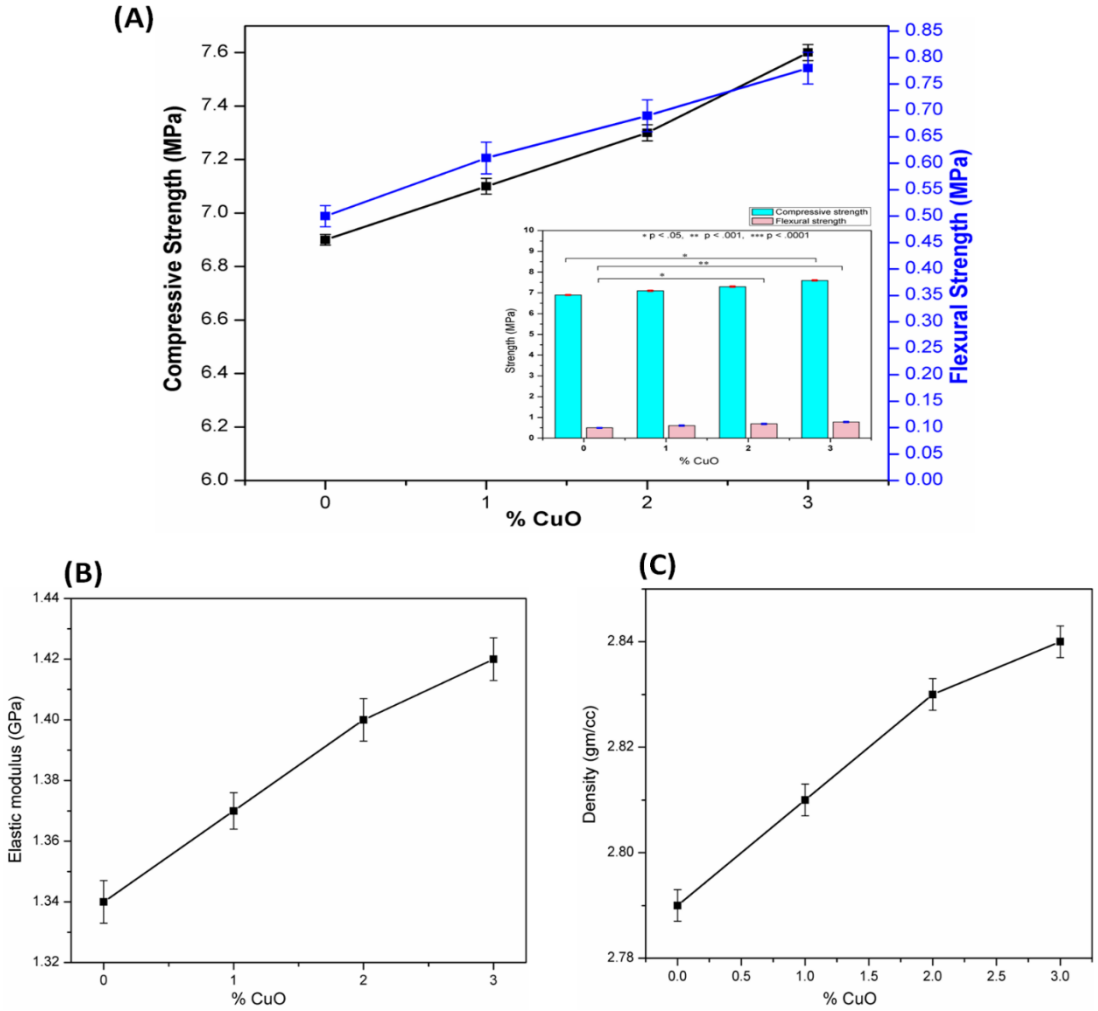

Fig 5.7 Change in **(A)** compressive and flexural strength **(B)** Modulus of elasticity after incorporation of copper into the parent glass system. **(C)** Density of as prepared melt derived annealed glass by Archimedes's principle. One way ANOVA using Tukey's post hoc test to perform significant ($p<.05$) and highly significant ($p<.01$ and $p<.001$) difference in mechanical properties ensures significant improvements in compressive and flexural strengths after Cu addition.

5.3.3 Chemical durability

Fig 5.8 represents the chemical durability of the glass scaffolds, expressed in terms of weight loss. The results indicate that, the weight loss percentage has increased with increasing copper oxide content in the 1393 glass scaffolds.

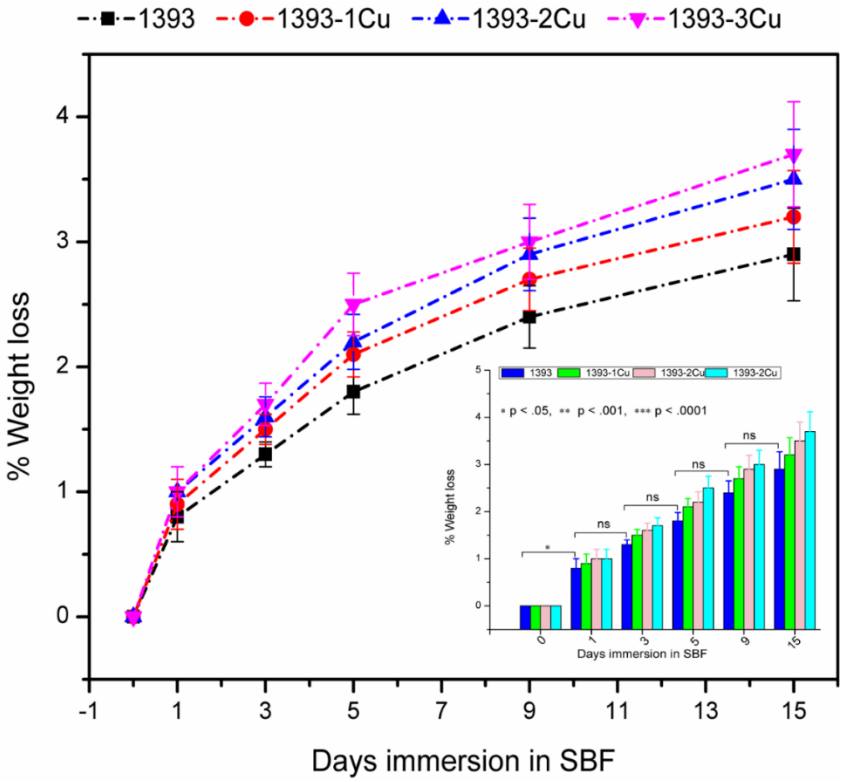

Fig 5.8 Chemical Durability of 1393 derived glass scaffolds as a function of material immersion time (days). Statistical analysis shows not significant (ns), significant (p<.05) and highly significant (p<.01 and p<.001) difference in pH and weight after Cu addition.

5.3.4 Assessment of biocompatibility

5.3.4.1 Cell viability

SCC-25 cells have been cultured on the bioactive scaffolds for cellular viability study. The results (Fig 5.9(B)) indicates that the viable cells after 48h of incubation and exposure on 1393 scaffold at concentrations of 5, 10, 25, and 50 mg/ml were 97.80%, 91.58%, 85.26% and 81.86% respectively. The cellular viability for 1393-1Cu and other copper substituted scaffolds at concentration 5 mg/ml were 96.03%, 96.98%, 95.71%. The cellular viability for 1393-2Cu at material concentrations of 5, 10, 20, 50 mg/ml were 97, 91, 84 and 79 %

respectively. The results (Fig 5.9(B)) illustrates the maximum viable cells for 1393 and 1393-2Cu while the viability is least for 1393-3Cu at lower material concentrations.

5.3.4.2 Cell proliferation

Fig 5.9(C) illustrates the cell proliferative study of SCC-25 after being cultured, incubated @ 37°C and exposed them to glass samples for 48h. Fig 5.9 (C) is the representation of the calculated cell proliferation of measured OD at 570nm. Cell proliferation has expressed in terms of growth inhibition. Result indicates that, the growth inhibition of 1393 for 50, 20, 10 and 5mg/ml material concentrations were 59.3%, 55.5%, 51.7% and 49.6%. The inhibition in 1393-3Cu were found to be 58.01%, 55.2%, 48.00% and 42.8% at the same material concentrations. However, the highest and lowest inhibition was observed respectively in 1393 and 1393-2Cu at low material concentrations.

5.3.4.3 Hemolysis assay

Fig 5.9(A) represents the percent hemolysis occurred when 1393 and their derivatives went through hemolysis assay. The assessment (Fig 5.9(A)) indicates the percentage of hemolysis occurred for 1393 scaffold were less than 2% (1.82) for 50mg/ml material concentration. Results also illustrate that the copper contained 1393 scaffold showing lower percentage of hemolysis upto 20mg/ml concentrations level than that of 1393. The percentage, although found almost similar at concentration of 50mg material to 1 ml of the blood.

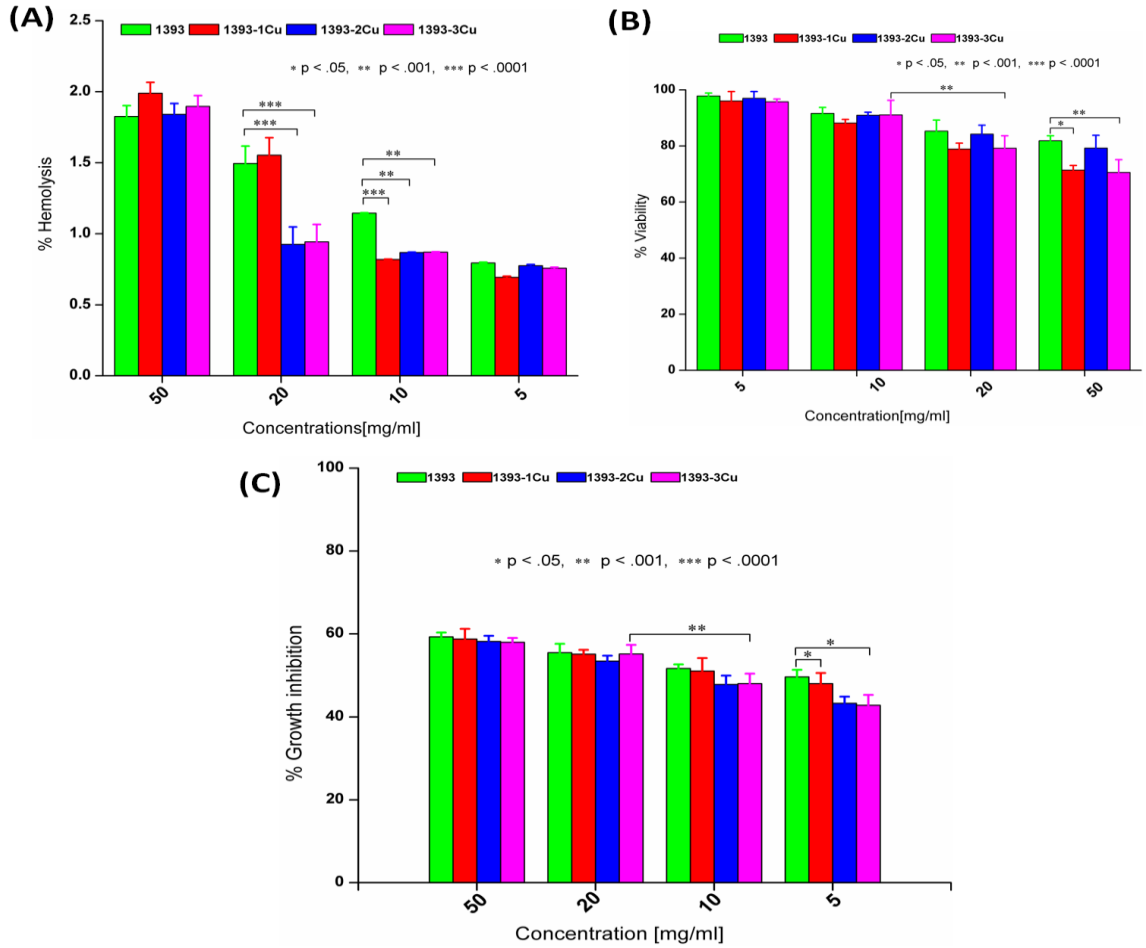

Fig 5.9 (A) Hemolysis assay of copper oxide containing 1393 glass scaffolds indicated in whole human blood with increasing CuO content. **(B)** Cell Viability and **(C)** Cellular Proliferation of 1393 bioactive glass scaffolds containing copper oxide against SCC-25 using MTT assay (Promega, USA), where 5×10^3 cells were plated in each of 96 well plates and were cultured in complete medium in bioactive glasses with different concentrations of the samples for 48h at 37 °C in 5% CO2. . One way ANOVA using Tukey's post hoc test to perform significant ($p<.05$) and highly significant ($p<.01$ and $p<.001$) difference in blood cell lysis, cellular viability and proliferation ensures significant reduction in hemolysis for 1393-2Cu @ 20mg/ml conc. and also better cell viability and proliferation for 1393-2Cu.

5.3.4.4 Apoptotic assessment

Apoptosis was determined by monitoring changes in the cell size and externalization of phosphatidylserine of the SCC-25 cells. The fluorescent images of the induced apoptosis shown in Fig 5.10 indicates the early apoptotic (Annexin FITC+/PI-), necrotic (Annexin FITC-/PI+) and the intact (Annexin FITC-/PI-) cells after 18 hours of incubation.

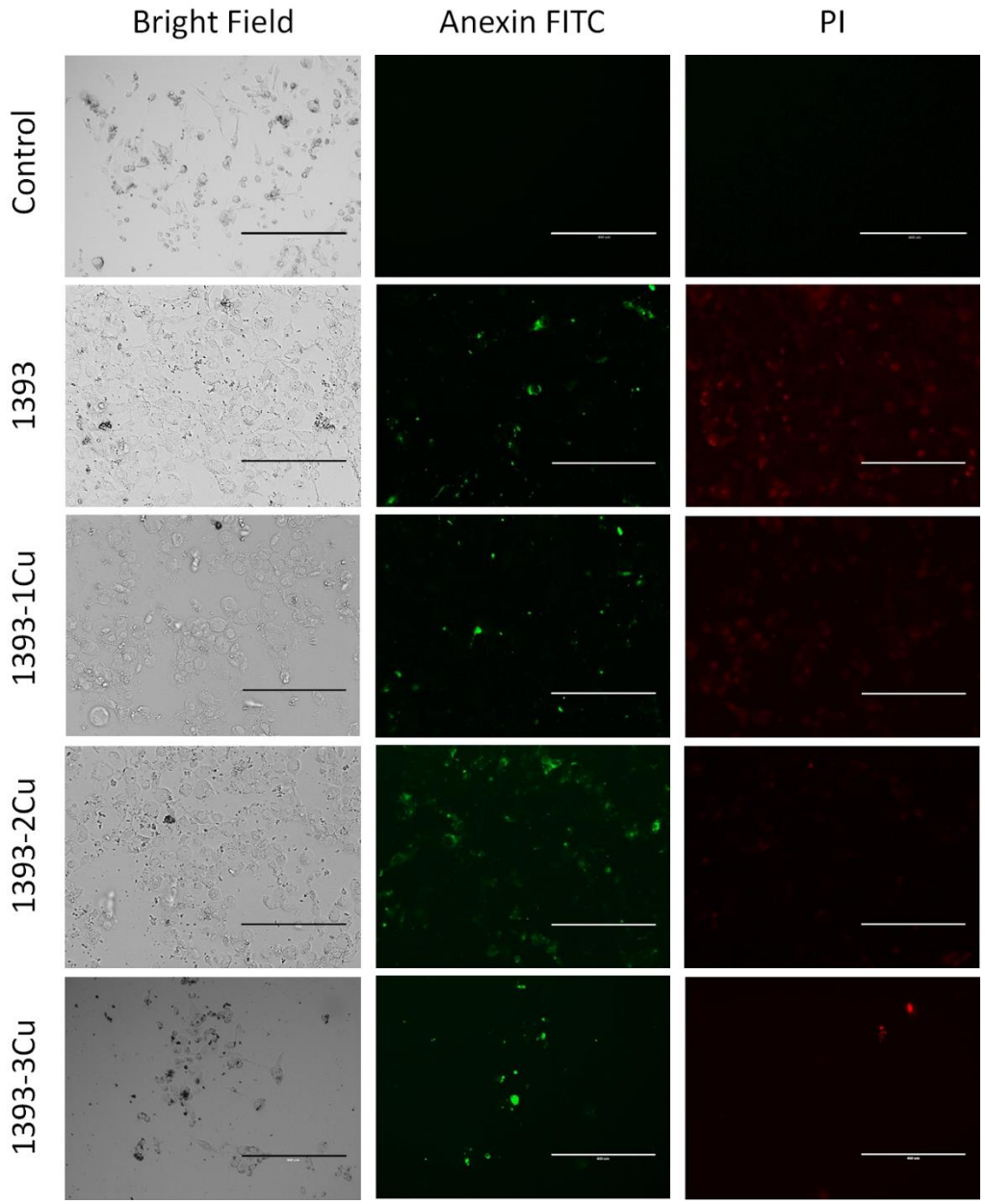

Fig 5.10 Fluorescent microscopic images of induced apoptosis after SCC-25 cells were treated with 100µg/ml of bioactive scaffolds (1393, 1393-1Cu, 1393-2Cu and 1393-3Cu) bioactive glasses in complete RPMI 1640 medium for 18 h @ 37 °C. Fluorescence microscope, Nikon Eclipse 80i (Nikon, Japan) with Plan Fluor 40×, NA 0.75 objective equipped with green (Annexin FITC) and red (Propidium Iodide) filters was used in

visualizing FITC-conjugated Annexin V and Propidium iodide (PI) stained apoptotic cells; n=3 (inside bar = 400µm).

5.4 Discussion

5.4.1 Evaluation of bioactivity

5.4.1.1 pH behavior in SBF

The mechanism of formation HCA can be estimated by pH behavior of SBF solution (Balamurugan et al., 2007, Arepalli et al., 2016, Fredholm et al., 2012). The rapid increase in pH can be inferred by the consumption of H^+ ions (or increase of OH^- ions) by means of dissolution and fast ion exchange of the cations from the surface of the scaffolds (like Na^{1+}, Ca^{2+}, K^{1+} etc) with H^+ and H_3O^+ present in SBF solution (Arepalli et al., 2015, Rahaman et al., 2011, Tripathi et al., 2015). The surface cations (Na^{1+}, Ca^{2+}, K^{1+}) of the bioactive glass scaffolds are believed to be removed easily because of increase of non-bridging oxygen (having lower bond strength than bridging oxygen bond strength) after addition of those network modifiers to the network former (SiO_2). Further, as the radius of those cations (Na^{1+} =102pm, Ca^{2+} =100pm, K^{1+} =138pm) are larger than the Si^{4+} (Si=100pm, Si^{4+}=40pm), their addition distorts and expands the normal glass network and eventually weaken the network structure (Brückner et al., 2016). Copper incorporation in the scaffolds was also found to increase the pH, as it could have facilitated enrichment of surface cations and their rapid dissolution as well (Stähli et al., 2015). The substitution of SiO_2 by CuO in 1393 scaffold is believed to have resulted in increase the alkali ions (Cu^{2+}, $Ca^{2+)}$ with respect to Si^{4+} in the subsequent scaffolds (1393-1Cu, 1393-2Cu, 1393-3Cu) which in turn, decreased the percentage of network former element (Si^{4+}) and increased NBO (non bridging oxygen). The higher NBO means lower bond strengths, hence lesser dissolution energy, so higher

release of ions and thus higher pH of the solution. Higher pH (basic in nature) led to attack the silica network and to form silanols (-SiOH) through hydrolysis (Hench, 1991). Continuous formation of silanols and their polymerization leads to form alkali ions (Na^+, Ca^{2+}) depleted silica rich layer. Further dissolution of the glass led to coupling the $Ca^{2+}$and PO_4^- ions from the solution, which in turn reduced the pH and promoted the HA like layer formation on the surface of the glass (Silver et al., 2001, Goel et al., 2011, Hoppe et al., 2011).

5.4.1.2 XRD

Bioactivity of the sample is associated with the ability to form HA (hydroxyapatite) like layer on their surface under physiological conditions. X-Ray diffraction analysis has long been used as a useful tool to determine the existence of HA on the surface of a sample. Here, in our investigation, we have observed that the intense peak found at 2θ =32° for all SBF treated scaffolds, corroborate the formation of HA layer which is matched with standard JSPDS, PDF# 74-0565 (Arepalli et al., 2016, Balamurugan et al., 2007) and the *sol-gel synthesized hydroxyapatite* itself (bottom curve) and also supported by pH, SEM and FTIR. The less intense peak at 2θ =45° could also be due to the formation of HA (PDF# 74-0566, 72-1243). Sharp peak at 2θ =32° for day5 samples can be described by the maximum formation of crystalline HA. The decrease in peak intensity for some curves can be attributed to the formation of some other minor phases. The broadened or less intense peak (Fig 5.3) for day9 and day15 samples may be due to the gradual conversion of crystalline hydroxyapatite [$Ca_{10}(PO_4)_6(OH)_2$] to nano (<150nm) size crystallites of hydroxycarbonate apatite (HCA) (Yan et al., 2001, LeGeros et al., 1965, Izquierdo - Barba et al., 1999) or formation of bioactive (or bioresorbable) amorphous TCP. From the results it is evident that, all the samples after immersion in SBF, confirms the HA layer formation,

hence they all are bioactive in nature. Furthermore, it is also evident from the figures, that the copper addition in the parent glass scaffold has no significant decrease in bioactivity. However, no sharp peaks for the as prepared scaffolds (Fig 5.2) even after sintering (at 700℃ for 12 hours) confirms the fewer tendency of devitrification of 1393 (Boyan et al., 1996, Deliormanlı, 2015). Also, the broad hump between 2θ=20-30° can be described by the fact that the scattered rays by atoms are not in a particular phase or direction. More specifically, they (the diffracted rays) scattered in many directions, leading to a large bump distributed in a wide range (2 Theta) instead of high intense narrower peaks, usually seen for glasses, emphasizes the retention of glassy nature of the 1393 bioactive glasses.

5.4.1.3 Surface morphology evaluation

The SEM micrographs (Fig 5.4) of SBF treated (15days @37℃) scaffolds (1393, 1393-1Cu, 1393-2Cu and 1393-3Cu) reveal the formation of HA like layer in the form of cluster at the surface of the scaffolds (Oyane et al., 2003). The formation of HA is also supported by XRD, FTIR analysis.Better HA layer formation for CuO incorporated scaffolds can be discussed by the phenomena of substitution of SiO_2 by CuO in 1393 scaffold, making the surface (1393, 1393-1Cu, 1393-2Cu) rich in alkali ions (especially Ca^{2+}), which could have led to higher adsorption of Ca^{2+} ions at the surface to facilitate better HA formation.

5.4.1.4 FTIR

The FTIR spectra of the bioactive scaffolds showed the changes that were in general conformity with the XRD analysis and the SEM observations. The result illustrates that there were trivial differences in the IR spectra of the four groups of SBF treated scaffolds while the differences are significant when in comparison to the ‘as fabricated’ scaffolds. The lowest spectral curve for each figure represents the as fabricated scaffold while the

other corresponds to SBF treated scaffold of the same species for different time periods. IR spectral resonances at 800-1250 cm^{-1} and 450 cm^{-1} for the as fabricated scaffold are attributed to the presence of Si-O-Si asymmetric stretching and bending vibrational group in the molecule. After immersion of the scaffolds for various days in SBF, the resonances of the Si-O-Si groups weakened distinctly and the resonances corresponding to vibrations of the PO_4^- group dominated the spectrum. The newer resonances are sometimes found to be overlapped with the preexisting resonances, (e.g.1030 cm^{-1} for P-O bending resonance overlapped with Si-O-Si asymmetric stretching in the wavenumber 800-1250 cm^{-1}. Furthermore, the spectral resonance at 560 cm^{-1} and 1030 cm^{-1} become visible after 1 day of immersion in SBF and gradually intense with the increasing number of soaking days confirms the formation of crystalline HA ($Ca_{10}(PO_4)_6(OH)_2$) layer (Deliormanlı, 2016, Lin et al., 2004, Lu et al., 2001).

5.4.2 Mechanical properties evaluation

Fig 5.7 (C) shows the density of the melt derived glass prior scaffoldings. The density of 1393 and other copper containing (1, 2, 3 mol%) glasses (not scaffold) measured by Archimedes's principle, were 2.79, 2.81, 2.82 and 2.84 respectively. Copper substitution for silicon may have resulted in increase in density as a result of replacement of lighter atoms (Si) by heavier one (Cu). Further due to the smaller size copper ions (ionic radius .72 Å) (Bejarano et al., 2015) can be interstitially located in as replacement proceeds which could lead to increase density of the glass.

From our observation, we found compressive and flexural strengths of 6.9 MPa and 0.5 MPa respectively for the 1393 scaffold which is lower than the maximum value reported by some researchers (Baino and Vitale - Brovarone, 2011, Fu et al., 2008). However,

statistical analysis of variance of mean (n=5) followed by Tukey's post hoc test affirms that, there was significant enhancement of compressive and flexural strength (Fig 5.7(A)) for some CuO derived scaffold than that of the parent one. Moreover, mechanical characterization of CuO doped 1393 based scaffold was not reported yet and thus the present work was done to evaluate mechanical properties of CuO doped 1393 scaffold. However, our developed CuO incorporated 1393 scaffold showed higher mechanical properties in comparison of previously reported mechanical strength (2.3 MPa) of CuO doped borate bioactive glass scaffolds (Wang et al., 2014). Also, an improvement in Elastic modulus of the scaffolds after CuO addition has been observed.

5.4.3 Chemical durability

From Fig 5.8, it was observed that percent weight loss of bioactive glasses increased with increasing copper oxide content in the scaffolds. Replacement of SiO_2 by CuO might have the potential in decreasing bridging oxygen (BO) as well as deformation of the normal SiO_4^- tetrahedra. With the decrease in BO (or increase in NBO), the glass structure become more open and thus increased the leachability of ions from the samples. Furthermore the stronger bond –Si-O-Si- could have replaced/modified with the weaker -Si-O-Cu- that might eventually weakened the network and led higher release of ions in the solution.

5.4.4 Cell viability, growth inhibition and cytocompatibility

It is worth mentioning that the untreated cells (control group) were considered as 100% viable or proliferative and 0% hemolytic. Based on this, the relative viability, proliferation or hemolysis was calculated in the experimental well. However, the results demonstrate that the maximum cellular viability was observed in 1393 and 1393-2Cu (Fig 5.9(B)) at

low concentrations of materials. Similarly, the minimal cellular inhibition was observed in 1393-2Cu at lower material concentrations (5.9(C)).

Nonetheless, the quantitative analysis indicates minimal cytotoxic nature of the materials and the intra group's cytotoxicity was found to be statistically insignificant even at higher material concentration. Moreover, the concentration dependent kinetic study indicates similar cytotoxic nature of the 1393-2Cu (2 mol% CuO incorporated scaffold) with the basal system (1393) due to their enhanced cytological compatibility than the other CuO incorporated glass systems. Meanwhile, the 1393-2Cu provided a better biological environment for SCC-25 cells to survive and grow than the other CuO incorporated glass.

5.4.5 Assessment of Hemolysis

Hemolysis is a destructive phenomenon where the destruction occurs in the red blood cells (RBC) when there are disorders in blood, which could be due to several reasons, e.g., foreign material comes in contact with blood and might be proven toxic. So, it is important to check the compatibility of materials to blood cells before clinical applications. The assessment (Fig 5.9(A)) indicates that the percentage of hemolysis that occurred in 1393 scaffolds was less than 2% at 50mg/ml material concentration, while the permissible limit is only 0.8%. Almost all scaffolds show less than the threshold value (0.8%) while the material concentration kept under 5 mg/ml. Statistical analysis of significance asserts better blood compatibility of CuO incorporated scaffolds than that of the basal system when the concentration was raised from 5 mg/ml to 20 mg/ml.

Meanwhile, the hemolysis assay has ascertained that the blood cells showed optimal compatibility (or minimal toxicity) in copper containing bioactive glasses compared to pure 1393. Herein, being an antimicrobial agent, copper in CuO incorporated glass system could

have diminished the harmful bacteria or other forms of microorganisms present in the blood cells.

5.4.6 Apoptotic assessment

Higher material concentrations raise the doubt of being cytotoxic and cause apoptosis is a matter of concern. However, the cytotoxic effect was due to necrotic cell death rather than apoptosis. Externalization of phosphatidylserine on the cell membrane was measured in the determination of apoptosis. Results indicate that the fluorescent microscopic images in early apoptotic cells (Annexin FIT+/PI) are green, necrotic cells (Annexin FITC-/PI+) are red, while viable cells didn't stain. Copper addition seems to reduce the apoptotic cell destruction up to a limit, which is also supported by literature (Rath et al., 2014), where up to 1% CuO was considered as non-cytotoxic.

5.5 Conclusions

Besides the facts that copper has a series of fascinating properties, the current investigation solely relies on studying the mechanical performance, *in vitro* bioactivity, and cellular metabolic activity of the CuO incorporated scaffolds. Here, we have successfully prepared the scaffold with the average porosity of >70%, (Fig 5.4(B)) (> 50% porosity is required for bone ingrowth). Moreover, the mechanical properties were appeared to be augmented in the post CuO incorporated scaffolds in comparison to the pure system. The mechanical strengths were, however, found similar to that of the trabecular bone (Liu et al., 2013b, Fu et al., 2011, Lewandrowski et al., 2002). Nevertheless, the *in vitro* cell culture study demonstrates their cytocompatibility and non-toxicity. Furthermore, the hemolysis assay ascertained optimal blood compatibility of the CuO substituted scaffolds. The apoptotic

assessment also confirmed reduced apoptosis in the copper containing bioactive glasses. Most importantly, the in vitro bioactivity assessment through XRD, SEM, FTIR, and pH, confirmed the HA formation over the glass surfaces. Although the in vitro tests make the CuO incorporated scaffolds a suitable candidate for neo bone tissue engineering application, the scaffolds should be examined further through in vivo tests to understand their reliability for clinical trials.